Pergamon

Int. J. Heat Mass Transfer. Vol. 38, No. 9, pp. 1675–1681, 1995

0017 9310/95 \$9.50+0.00

0017–9310(94)00284–3

# A mathematical model for the prediction of heat transfer from finned surfaces in a circulating fluidized bed

P. K. NAG, M. NAWSHER ALI† and P. BASU‡

Department of Mechanical Engineering, Indian Institute of Technology, Kharagpur-721302, India

(*Received* 29 *January* 1994 *and in final form* 10 *August* 1994)

**Abstract**—A mathematical model has been developed to predict heat transfer coefficients on projected finned surfaces in a circulating fluidized bed (CFB). To validate the model, experiments were conducted in a 100 mm i.d., 5.15 m high CFB unit, in which heat transfer coefficients were measured for fins having rectangular and pin shapes. Experiments covered a range of superficial velocity from 5.6 to 11.4 m s$^{-1}$, bed temperature from 66.5 to 91.5°C and for 310 μm sand particles. Heat transfer coefficients predicted from the model have been compared with those experimentally obtained and a good agreement is observed.

## INTRODUCTION

The mechanism of heat transfer in a circulating fluidized bed (CFB) is complex because of the dependence of bed behaviour on a large number of variables. The process of heat exchange between the system and the heat transfer surface is closely related to the process of heat transfer between the fluidized solids and the fluidizing gas, the rate of mixing of particles in the bed, and the geometry of the fluidized bed. The fluidized bed represents a complex interaction of gas and solid. In addition, the radial variation of bed density complicates the development of a fundamental model for the prediction of heat transfer at the wall, especially when fins are attached to the inner surface of the bed.

Finned tubes are widely used in heat exchangers. In a CFB boiler, the heat absorption by each wall tube may be considerably increased if additional heating surfaces can be provided by welding vertical fins to each tube. Tung *et al.* [1], Li *et al.* [2] and many others have observed a dilute core of solids accompanied by a dense wall region in a CFB. So, the heat transfer coefficient along the fin surface varies as the fin extends from the wall towards the centre of the bed. To the best of the authors' knowledge no model for the prediction of heat transfer for the finned surface in a CFB has yet been published in the literature. In the present paper an analytical model has been proposed for predicting heat transfer in a circulating fluidized bed with finned surface. It has been validated by conducting experiments in a CFB facility developed for the investigation. This being the first attempt, the analysis is limited to temperatures where radiation is negligible. Radiation will be considered later in the model when experimental data from high temperature beds will be used for its validation.

† On leave from Bangladesh Institute of Technology, Khulna, Bangladesh.

‡ Technical University of Nova Scotia, Halifax, Canada B3J 2X4.

## MODEL

Assuming that a cluster of particles from the bulk of the bed moves to the heated finned surface, receives heat from the wall, and then moves away from the surface, and neglecting radiation, the temperature distribution along the fin (Fig. 1) is given by the following differential equation [6]:

$$\frac{d^2T}{dx^2} = \frac{Ph_x}{kA}(T - T_b). \quad (1)$$

Let $x$ be the axial coordinate with its origin at the tip so that $(x/L)_{tip} = 0$ and $(x/L)_{base} = 1$ and the fin lies in the region $0 \leqslant x/L \leqslant 1$.

It is assumed that the fin is sufficiently long so as to neglect the tip loss, but being long it will be subjected to radial distribution of suspension density in the fast bed. Glicksman [3] and Basu [4] observed that, for small beds (< 15 cm diameter), the heat transfer coefficient varies approximately with the square root of cross-section average suspension density. In the present analysis, however, it has been assumed that $h_x = k'\sqrt{\rho_x}$, where $k'$ is an experimentally determined constant and $\rho_x$ is the local suspension density varying linearly along the fin length so that

$$\rho_x = \rho_h + \frac{x}{L}(\rho_w - \rho_h) \quad \text{and} \quad \bar{\rho} = \frac{\rho_w + \rho_h}{2},$$

which on substitution in equation (1) gives

$$\frac{d^2T}{dx^2} = \frac{\rho k'}{kA}\left[\rho_h + \frac{2x}{L}(\rho_w - \bar{\rho})\right]^{1/2}(T - T_b). \quad (2)$$

## NOMENCLATURE

| | |
|---|---|
| $A$ | cross-sectional area of fin [m$^2$] |
| $A_b$ | bare surface area [m$^2$] |
| $A_T$ | total heat transfer area [m$^2$] |
| $A_F$ | surface area of fins [m$^2$] |
| $A_{UF}$ | area of unfinned surface [m$^2$] |
| $d_p$ | particle diameter [mm] |
| $h$ | average overall heat transfer coefficient [W m$^{-2}$ K$^{-1}$] |
| $h_F$ | heat transfer coefficient from finned surface [W m$^{-2}$ K$^{-1}$] |
| $h_{UF}$ | heat transfer coefficient from unfinned surface [W m$^{-2}$ K$^{-1}$] |
| $h_T$ | predicted heat transfer coefficient [W m$^{-2}$ K$^{-1}$] |
| $h_x$ | local heat transfer coefficient [W m$^{-2}$ K$^{-1}$] |
| $I$ | current [A] |
| $k$ | thermal conductivity of fin material [W m K$^{-1}$] |
| $k'$ | experimentally determined constant |
| $l, L$ | height of fin from the wall [m] |
| $L_p$ | distance between pressure tappings [m] |
| $m$ | fin parameter, $\sqrt{hP/kA}$ |
| $N_f$ | number of fins |
| $P$ | perimeter [m] |
| $q''$ | heat flux [W m$^{-2}$] |
| $Q_T$ | total heat transfer [W] |
| $Q_F$ | heat transfer from finned surface [W] |
| $Q_{UF}$ | heat transfer from unfinned surface [W] |
| $r$ | local radius [m] |
| $R$ | radius of column [m] |
| $Re_p$ | particle Reynolds number, $U_0 d_p \rho_g/\mu_g$ |
| $T$ | local temperature [K] |
| $T_b$ | bed temperature [K] |
| $T_w$ | surface or wall temperature [K] |
| $U_0$ | superficial velocity [m s$^{-1}$] |
| $V$ | voltage [V] |
| $x$ | distance from the fin tip [m]. |

Greek symbols

| | |
|---|---|
| $\varepsilon$ | cross-section average voidage fraction |
| $\mu_g$ | viscosity of gas [kg m$^{-1}$ s$^{-1}$] |
| $\eta_{fin}$ | fin efficiency |
| $\rho$ | average suspension density [kg m$^{-3}$] |
| $\rho_h$ | suspension density at the fin tip [kg m$^{-3}$] |
| $\rho_w$ | suspension density at the wall [kg m$^{-3}$] |
| $\rho_x$ | local suspension density [kg m$^{-3}$] |
| $\rho_g$ | density of gas [kg m$^{-3}$] |
| $\rho_s$ | density of solid [kg m$^{-3}$] |
| $\rho_{sus}$ | suspension density [kg m$^{-3}$] |
| $\theta$ | temperature difference [K] |
| $\theta_0$ | temperature difference at the fin base [K]. |

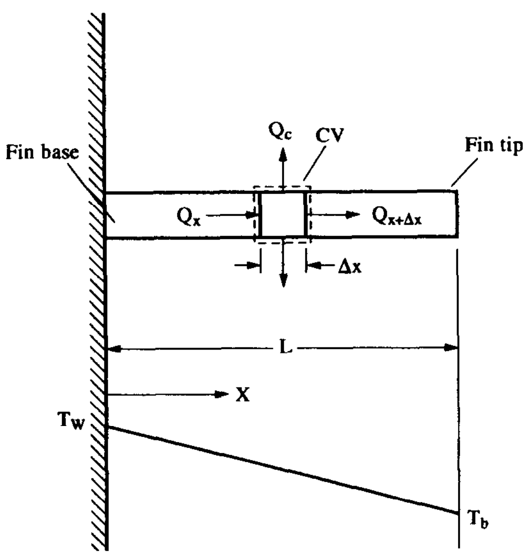


Fig. 1. Nomenclature for the derivation of one-dimensional fin equation.

The local suspension density $\rho_x$ is estimated from the radial voidage distribution given by Tung *et al.* [1]:

$$\varepsilon(r) = \varepsilon^{[3.62(r/R)^{6.75}+0.191]} \qquad (3)$$

where $\varepsilon$ is the cross-section average voidage fraction. At the wall, $r = R$ and $\varepsilon_w = \varepsilon^{3.811}$ and $\rho_w = \rho_s(1-\varepsilon_w)+\rho_g\varepsilon_w$, and at the fin tip $\varepsilon_h = \varepsilon^{[3.62(R-L/R)6.75+0.191]}$ and $\rho_h = \rho_s(1-\varepsilon_h)+\rho_g\varepsilon_h$, $L$ being the fin length.

Equation (2) is now transformed to

$$\frac{d^2\theta}{dx^2} = C^2(\sqrt{a+bx})\theta \qquad (4)$$

where $\theta(x) = T(x)-T_b$, $C^2 = \rho k'/kA$, $a = \rho_h$ and $b = 2/L(\rho_w-\bar{\rho})$.

It is valid for $0 \leqslant x/L \leqslant 1$ and subject to the conditions of

$$\theta(x) = T_w - T_b = \theta_0 \quad \text{at} \quad x/L = 1 \qquad (5)$$

$$\frac{d\theta(x)}{dx} = 0 \quad \text{at} \quad x/L = 0. \qquad (6)$$

Substituting $U = a+bx$, equation (4) takes the form of

$$\frac{d^2\theta}{dU^2} - m'^2\sqrt{U}\theta = 0 \qquad (7)$$

where $m' = C/b$. It is a form of Bessel's equation, and, following Arpaci [5], it is solved with the help of boundary conditions, equations (4) and (5), as given below:

$$\frac{\theta(x)}{\theta_0} = \frac{\sqrt{(a+bx)}\, I_{-2/5}(\frac{4}{5}m'(a+bx)^{5/4})}{\sqrt{(a+b)}\, I_{-2/5}(\frac{4}{5}m'(a+bL)^{5/4})}. \quad (8)$$

This is the final expression for temperature distribution along the fin length.

Now, the heat input to each fin (Fig. 1) is given by

$$Q_{\text{fin}} = -\left(-kA\frac{d\theta}{dx}\right)x = L. \quad (9)$$

Differentiating equation (8) with respect to $x$, putting the limit $x = L$, and substituting in equation (9), the following equation is obtained:

$$Q_F = \frac{N_f\theta_0\sqrt{Pk'Ak}(U^{3/4})(I_{3/5}(4/5m'U^{5/4}))}{\sqrt{\rho_w}\,(I_{-2/5}(4/5m'\rho_w^{5/4}))} \quad (10)$$

where $N_f$ is the number of fins. The total heat transfer, $Q_T$, from a finned surface thus becomes

$$Q_T = Q_F + Q_{UF}. \quad (11)$$

The average overall heat transfer coefficient is obtained on dividing equation (11) by $\theta_0$ and $A_T$ as given below:

$$h_T = \frac{N_f\sqrt{Pk'Ak}\,(U^{3/4})(I_{3/5}(\frac{4}{5}m'U^{5/4}))}{A_T\sqrt{\rho_w}\,(I_{-2/5}(\frac{4}{5}m'\rho_w^{5/4}))} + \frac{A_{UF}}{A_T}(q''/\theta_0). \quad (12)$$

Heat transfer data on CFB with fins not being available, the heat transfer coefficients predicted from the model have been compared with those of present experiments.

## EXPERIMENTAL FACILITY

The CFB unit [Fig. 2(a)] in which experiments were conducted comprised a 100 mm i.d., 5.15 m high main column, made up of steel sections, along with a return leg, mainly made up of plexiglass, a cyclone and a bag filter. Air was supplied by a high-pressure centrifugal blower, and the air flow rate, regulated by an air control valve and a bypass arrangement, was measured by a standard orifice meter. The distributor plate of 6 mm thickness made of mild steel was a straight hole orifice type having hole diameter 3 mm, pitch 8 mm and 138 holes. This provided 12.4% opening area for air flow. A butterfly valve was located about midway in the return leg to measure the solid circulation rate in the column by rapidly closing the valve and measuring the volume of solids collected above it over a certain period of time. Entrained solids were recovered in a cyclone and returned through the downcomer to the bottom of the main column by aeration air. The solids return point was located 0.5 m above the distributor. Static pressures were measured at 0.5 m intervals along the bed height. Fine wire mesh (British Standard 400) and cigarette filters were used at the ends of pressure taps to minimize pressure fluctuations in the water-filled manometers.

The test section [Fig. 2(b)], 300 mm long, was located 2.75 m above the distributor. A 1240 W tape heater was wrapped uniformly around it. It was then insulated with glass wool and asbestos rope. Asbestos gaskets of about 10 mm thickness were used at the flanges. Two guard tape heaters were provided before and after the test section to prevent axial heat loss by conduction along the pipe wall by controlling the surface temperatures of guard heaters recorded by thermocouples so as to match them to the temperature of the test section. Electrical energy input to the heater was controlled by a variac and measured with a voltmeter and an ammeter. The temperatures of the inside wall and of the bed at about the mid-point in the test section were measured with copper–constantan thermocouples. The thermocouple wires were all connected to a multi-point switch and then to a digital d.c. microvoltmeter.

Experiments were first conducted with the test section having no fins. Then these were repeated for two-, four- and eight-rectangular and 16- and 32-pin finned surfaces. Two, four and eight vertical rectangular fins (246 × 23 × 6 mm) were located at 180, 90 and 45° apart, respectively. These fins were tightly screwed to the wall and special care was taken to ensure near perfect contact of the fin with its base. The pin fins (6.35 mm dia. × 15 mm long) were fitted to the test section by screwing. Sixteen-pin fins were fitted in four rows and four columns in such a manner that the columns were at 90° apart and the rows were equidistant. Thirty-two-pin fins were fixed in the same manner, except that the columns were at 45° apart. Local sand of mean diameter ($d_p$) 310 μm was used as the bed material. The experimental conditions are given in Table 1.

## RESULTS AND DISCUSSION

The average heat transfer coefficient ($h$) was determined for each operating condition at steady state from the measured heat flux and the temperatures of the inside wall of the riser ($T_w$) and the bed suspension ($T_b$)

$$h = VI/A_b(T_w - T_b) \quad (13)$$

where $V$ and $I$ are the voltage and current, respectively, and $A_b$ is the total surface area of the bare (unfinned) test section. When fins were incorporated, the total heat transfer was estimated from the relation [6]

$$\begin{aligned} Q &= \text{heat transfer from unfinned surface} \\ &\quad + \text{heat transfer from finned surface} \\ &= h(T_w - T_b)A_b + h(T_w - T_b)A_f\eta_{\text{fin}} \quad (14) \end{aligned}$$

where $A_F$ is the surface area of the fins and $\eta_{\text{fin}}$ is the

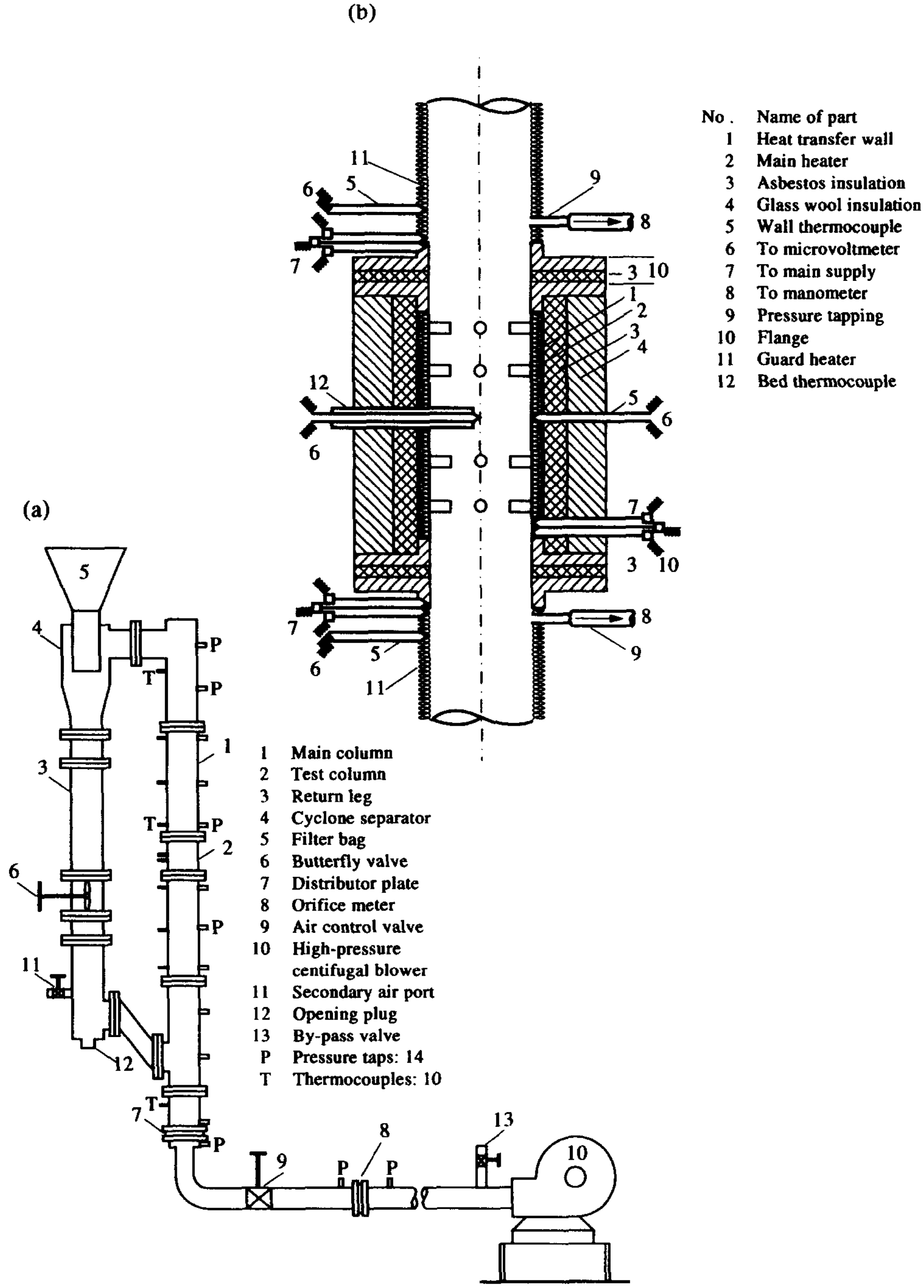


Fig. 2. (a) Schematic diagram of experimental set-up. (b) Finned test section.

fin efficiency. The heat input to the test section was maintained constant with the help of a variac.

The fin efficiency which provides a quantitative measure of its thermal performance is defined as

$$\eta_{\text{fin}} = \frac{\text{actual heat transfer through the fin}}{\text{ideal heat transfer through the fin}}.$$

Ideal heat transfer occurs when the heat transfer coefficient is uniform over the entire finned surface at the unfinned surface value and when there is no thermal resistance within the fin, the entire fin surface being maintained at the base temperature $T_w$. For a long and thin pin when tip loss is neglected, $\eta_{\text{fin}}$ is given by [7]

$$\eta_{\text{fin}} = \frac{\tanh ml}{ml} \tag{15}$$

where for a pin $m = [(h/kD)]^{1/2}$, $D$ being the diameter of the pin. Similarly, it was derived for a rectangular fin [7, 8].

The bed voidage ($\varepsilon$) in the test section was estimated

Table 1. Experimental conditions

| | |
|---|---|
| 1. Mean particle size | $d_p = 310\ \mu$ |
| 2. Density of sand | $\rho_s = 2350$ kg m$^{-3}$ |
| 3. Minimum fluidization velocity | $U_{mf} = 0.075$ m s$^{-1}$ |
| 4. Voidage at $U_{mf}$ | $\varepsilon_{mf} = 0.5$ |
| 5. Terminal velocity | $U_T = 1.54$ m s$^{-1}$ |
| Variable | Range |
| Fluidizing velocity [m s$^{-1}$] | 5.6–11.4 |
| Bed temperature [K] | 340–365 |
| Suspension density [kg m$^{-3}$] | 18–76 |
| Heat flux [W m$^{-2}$] | 3580–7876 |
| Bed inventory [kg] | 20–32 |
| Mode of heating | Electric heater |
| Fin geometry | Rectangular and pin shaped |

from the pressure drop ($\Delta p$) measured by a water filled U-tube manometer connected across it:

$$\varepsilon = 1-(\Delta p/\rho_s L_p g). \tag{16}$$

The suspension density of the bed was determined from the relation

$$\rho_{sus} = \rho_s(1-\varepsilon)+\rho_g\varepsilon. \tag{17}$$

The particle Reynolds number $Re_p$ is defined as

$$Re_p = (U_0 d_p \rho_g)/(\mu_g). \tag{18}$$

Heat transfer data for finned surfaces not being available, the present experiments were first performed with unfinned surfaces and the results were compared with those of some previously published data [8]. Then the predicted results from the model have been compared with those of the present experiments with two-, four- and eight-rectangular, and 16- and 32-pin finned surfaces. These latter results, together with the performance of fins in CFB, are shown in Figs. 3–8.

A measure of fin tube performance is the ratio of the heat transfer coefficient for a finned surface compared to that obtained on an unfinned surface under identical CFB conditions. When this ratio is unity, exceeds unity or even just a substantial fraction of unity, one may expect the finned tube to provide higher heat transfer duty per unit length than an unfinned surface [9]. Figure 3 shows a plot of this ratio ($h_F/h_{UF}$) as a function of particle Reynolds number ($Re_p$). Data taken from three test sections having different fin gaps have been plotted in this figure. Each curve represents the result obtained for a particular finned test section, operating with the same fluidized condition and the same particle size. Some interesting points are indicated by these graphs. First, one can look at the value of the coefficient ratio, which is relatively high, being above 0.65 for the great majority of the cases and, in fact, for one of the finned tube test sections, the coefficient ratio approaches unity ($>0.9$). Second, from a comparison of the three curves, it is evident that increasing fin count, i.e. decreasing fin gap, causes a definite decrease in the ratio of heat transfer coefficients. Third, it is evident that the heat transfer coefficient ratio decreases with $Re_p$ or superficial velocity. As the number of fins is increased, the solid movement becomes restricted. In addition, with the increase of superficial velocity, the solids are swept away from the test section. Thus, the suspension density is decreased, resulting in lower heat transfer coefficient ratio.

The capacity function ($A_F h_F/A_{UF} h_{UF}$) is a direct measure of the heat transfer capability for a finned surface relative to an unfinned surface occupying the

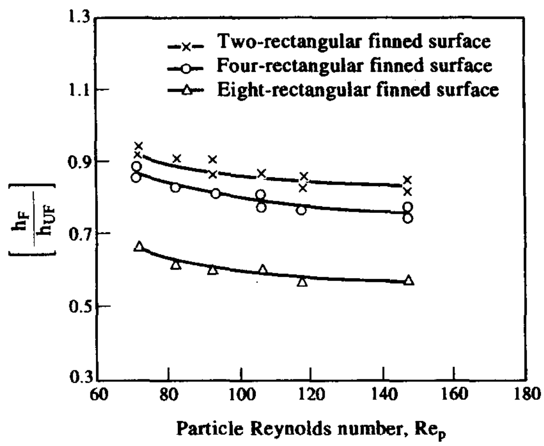


Fig. 3. Effect of $Re_p$ on the ratio of heat transfer coefficients for finned and unfinned surfaces.

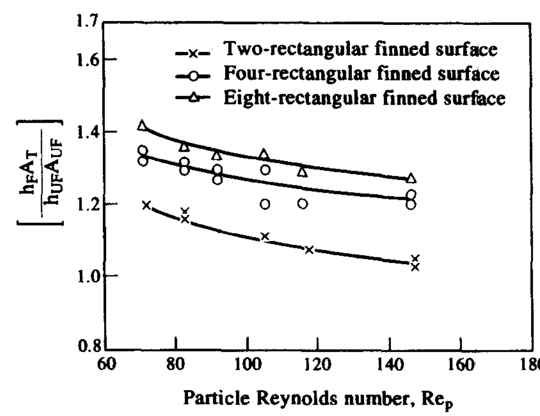


Fig. 4. Effect of $Re_p$ on capacity function.

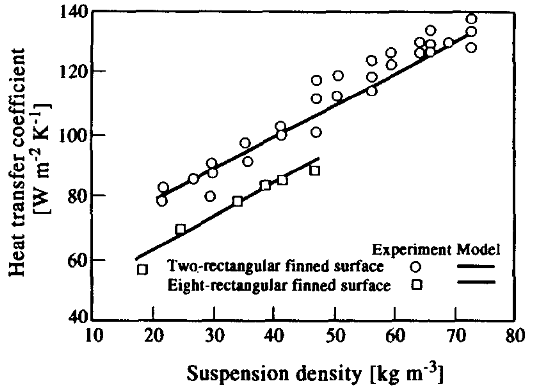


Fig. 5. Comparison of predicted values from the model with experimental results for two- and eight-rectangular finned surfaces.

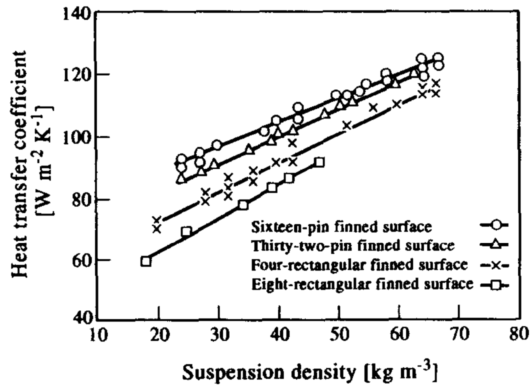


Fig. 8. Variation of heat transfer coefficient predicted from the mathematical model with suspension density.

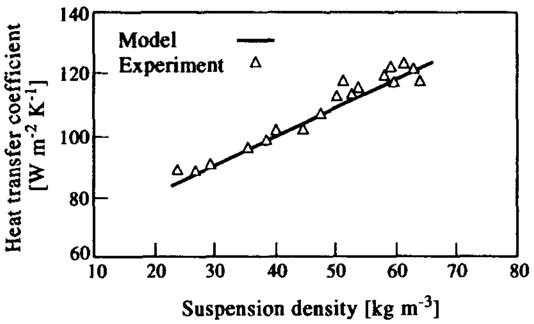


Fig. 6. Comparison of predicted values from the model with experimental results for 32-pin finned surface.

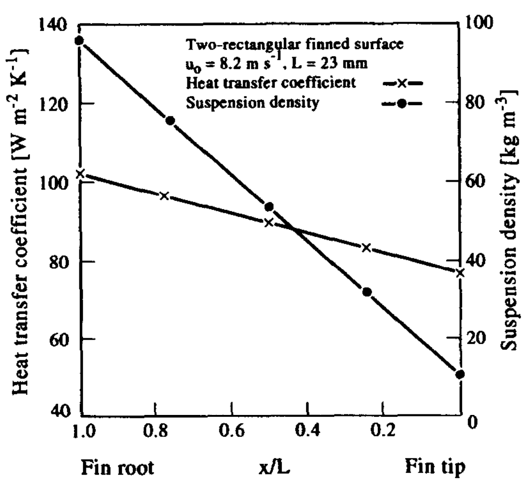


Fig. 7. Variation of computed heat transfer coefficient and suspension density from the root to the tip of the fin (from mathematical model).

same superficial bed volume. Figure 4 is a diagrammatic representation of this function, as found for the various finned surfaces tested in this investigation. For each finned surface, the capacity function is plotted against the particle Reynolds number with the fin count as the other variable. It is observed that, with the increase in the number of fins, i.e. with the increase of heat transfer area, the curve shifts to the top, as expected. For the conditions represented in Fig. 4, the values of the average capacity functions were approx. 1.1, 1.25 and 1.32 for two-, four- and eight-rectangular finned surfaces, respectively. This represents a substantial increase in heat transfer capability over the unfinned surface of the order of 25–103% [8].

Heat transfer coefficients predicted from the model and the experimentally determined values for two- and eight-rectangular and 32-pin finned surfaces are plotted against suspension density in Figs. 5 and 6 respectively, which demonstrates fair agreement. For all the cases, it is observed that the heat transfer coefficient increases monotonically with the increase in suspension density as is found for unfinned surfaces. As the solid particles come randomly into contact with the heat transfer surface, there is transient heat conduction which is the dominating mode of heat transfer between the fluidized bed and the wall. More suspension density means more particles per unit volume and, hence, the heat transfer coefficient is higher for a greater suspension density. It is further observed that, with the increase in the number of fins, i.e. with the decrease in fin spacing, the heat transfer coefficient decreases. It happens due to the fact that the fins obstruct the downward movement of solid particles, resulting in the reduced suspension density and increased voidage at the test section, which is attributed to lower values of the heat transfer coefficient. Priebe and Genetti [10] and Chen and Withers [9] also observed reduction in heat transfer coefficient when fins were used on tubes immersed in bubbling fluidized beds.

The distribution of suspension density and heat transfer coefficient along the surface of the fin, extended into the bed, are plotted in Fig. 7. Both suspension density and heat transfer coefficient were predicted from the model at five equidistant points along the fin surface. The dimensionless parameter fin length ($x/L$) is taken as zero at the fin tip and unity at the fin base. It is observed from the plot that both suspension density and heat transfer coefficient decrease from the fin base (wall) to fin tip, indicating a maximum value at the bed wall (fin base), and then linearly decreasing towards the centre of the bed. This fact is supported by the experimental observations of many workers [1, 2].

The predicted heat transfer coefficients from the model for 16-, 32-pin finned, and four- and eight-rectangular finned surfaces have been plotted against suspension density in Fig. 8. A monotonic increase in heat transfer coefficient with suspension density for all the curves is observed, as expected. It is further observed that, with the increase in the number of fins, the curve shifts downward, showing lower values of the heat transfer coefficient both for pin and rectangular finned surfaces, which agrees fairly well with the present experimental results.

## CONCLUSION

The inferences drawn from the investigation can be summarized as follows:

(1) Heat transfer from fins in circulating fluidized beds can be predicted from the analytical model proposed here.

(2) Bed-to-wall heat transfer increases with increasing suspension density.

(3) Addition of fins decreases the heat transfer coefficient. The heat transfer coefficients for finned tube are generally in the range of 0.68–0.90 times that of bare tubes under similar fluidized conditions.

(4) An increase in the number of fins decreases the heat transfer coefficient. However, it increases the total heat transfer.

(5) Both suspension density and heat transfer coefficient decrease along the surface from the base towards the tip of the fin, as predicted from the present model.

## REFERENCES

1. Y. Tung, J. Li and M. Kwauk, Radial voidage profiles in fast fluidized beds. In *Fluidization* (Edited by M. Kwauk and D. Kunii), pp. 139–145. Science Press, Beijing (1988).
2. J. Li, Y. Tung and M. Kwuak, Axial voidage profiles in fast fluidized beds in different operating regions. In *Circulating Fluidized Bed Technology*—II (Edited by P. Basu and J. F. Large), pp. 193–203. Pergamon Press, Oxford (1988).
3. L. R. Glicksman, Heat transfer in circulating fluidized beds. In *Circulating Fluidized Bed Technology*—II (Edited by P. Basu and J. F. Large), pp. 13–29. Pergamon Press, Oxford (1988).
4. P. Basu, Heat transfer in high temperature fast beds. *Chem. Engng Sci.* **45,** 3123–3136 (1990).
5. V. S. Arpaci, *Conduction Heat Transfer*. Addison-Wesley, London (1966).
6. F. Kreith and M. S. Bohn, *Principles of Heat Transfer*, 4th Edn. Harper & Row, New York (1986).
7. M. N. Ozisik, *Heat Transfer—a Basic Approach*, 3rd Edn. McGraw-Hill, New York (1988).
8. P. K. Nag and M. N. A. Moral, The influence of rectangular fins on heat transfer in circulating fluidized beds. *J. Inst. Energy Lond.* **63,** 143–147 (1990).
9. J. C. Chen and J. G. Withers, An experimental study of heat transfer from plain and finned tubes in fluidized beds. *A.I.Ch.E. Symp. Ser.* No. 174, **74,** 327–333 (1978).
10. S. J. Priebe and W. E. Genetti, Heat transfer from a horizontal bundle of extended surface tubes to an air fluidized bed. *A.I.Ch.E. Symp. Ser.* **73,** 38–43 (1977).